Numerical Study on the Vertical Bridgman Crystal Growth with Thermosolutal Convection

Moo Geun Kim

School of Mechanical and Automotive Engineering, Inje University, Kyungnam 621-749, Korea

Geun Oh Kim, Byung Kyu Park*

Department of Thermal, Fluid, and Environmental Engineering, Korea Institute of Machinery and Materials, Taejon 305-343, Korea

A numerical analysis has been carried out to investigate the influences of thermosolutal convection on the heat and mass transfer and solute segregation in crystals grown by the vertical Bridgman technique. The governing equations are solved by a finite-volume method using the power law scheme and the SIMPLE algorithm in which body-fitted coordinate system has been used. A primary convective cell driven by thermal gradients forms in the bulk of the domain, while a secondary convective cell driven by solutal gradients forms near interface. As the solutal Rayleigh number increases, secondary cell becomes to be stronger and has a great influence on the radial concentration along the interface.

Key Words : Thermosolutal Convection, Solidification, Melt-Solid Interface, Bridgman Crystal Growth

Nomenclature

C_0 : Average solute concentration [wt. %]
C_p : Specific heat [kJ/kgK]
D : Solutal diffusivity [m^2/s]
g : Gravity [m/s^2]
h : Heat transfer coefficient [W/m^2K]
k : Segregation coefficient
k_s : Thermal conductivity of solid [W/mK]
k_m : Thermal conductivity of melt [W/mK]
Pr : Prandtl number
P : Pressure [N/m^2]
R : Radius of ampoule [m]
Ra_T : Thermal Rayleigh number
Ra_S : Solutal Rayleigh number
Sc : Schmidt number
T : Temperature [K]
u, v : Velocity [m/s]

Greek symbols

α : Thermal diffusivity [m^2/s]
β_T : Thermal expansion coefficient [K^{-1}]
β_S : Solutal expansion coefficient [wt. $\%^{-1}$]
ε : Emissivity of surface
ρ : Density [kg/m^3]
ν : Kinematic viscosity [m^2/s]
σ : Stefan-Boltzmann constant [W/m^2K^4]
ψ : Stream function

Subscripts

c : Cold zone
h : Hot zone
L : Melt
m : Melting point
S : Solid

* Corresponding Author,
E-mail : bkpark@kimm.re.kr
TEL : +82-40-868-7367; **FAX** : +82-42-868-7335
Department of Thermal, Fluid, and Environmental Engineering, Korea Institute of Machinery and Materials, Taejon 305-343, Korea.(Manuscript **Received** February 2, 2001; **Revised** May 8, 2001)

1. Introduction

The quality of semiconductor crystals grown from the melt can be influenced by the thermal and chemical transport phenomena that occur in the melt. The primary transport mechanism is natural convection.

The convection in turn produces horizontal gradients in the solute fields of the melt and the resulting crystal exhibits solute segregation along the interface. With diffusion of both temperature and solute in the melt, the fluid is subject to thermosolutal or double-diffusive instabilities.

To obtain a high quality crystal with this system, compositional uniformity along the melt -solid interface is required. In addition the shape of the melt-solid interface is one of the important factors, which influences the crystalline quality.

Usually it is desirable to suppress convection throughly, and to maintain a planar melt-solid interface with gradients of temperature and concentration perpendicular to the interface. In this case both the temperature and concentration are uniform along the interface, and the solute that is incorporated in the crystals is distributed homogeneously. A solute boundary layer forms in the melt adjacent to the interface. This transient solute layer determines the magnitude of solutal convection. In turn, the flow velocities influence the solute distribution by convective transport.

A more complete understanding of the effects of heat transfer, melt convection on interface shape, and segregation would certainly help to improve the quality and yield.

During the last decades, general understanding of interaction between the transport and the crystal growth process has improved substantially. Although, the quantitative prediction of solidification phenomena within the melt is not clearly revealed.

Many simulations of Bridgman crystal growth processes are available in the literatures. The influence of natural convection and the interface curvature on radial segregation has been studied by Chang et al.(1983) using the finite element method, but the convection due to solutal gradients was not included. Also Carlson et al. (1984) has conducted a numerical simulation to study thermally driven flows of a pure melt during vertical Bridgman crystal growth. Since they ignored the presence of solute, only thermal convection was considered and no quantitative result for solute segregation in the solid was provided. Recently, some authors (Ouying and Shyy, 1997; Kuppurao and Derby, 1997) have carried out the numerical analysis to evaluate the interface shape, position during the crystal growth using the vertical Bridgman technique. Xing et al. (1996) have developed a thermosolutal convection model to simulate the heat, solute and fluid flow fields in the melt. However, those studies have principally analyzed the influence of thermal convection on the fluid flow. Much less attention was given to the effect of convection on the interface shape.

Several analytical (Dutta et al., 1995) and 3-D numerical analyses (Xiao et al., 1996) have been carried out to include a variety of complicated factors for the Bridgman configuration. However, the analysis of vertical Bridgman crystal growth with consideration of thermo-solutal convection and interface shape has not been carried out in detail.

In this study a computational model is applied to simulate the solidification process of the gallium doped with germanium in vertical Bridgman configuration and nonlinear numerical computation was carried out in order to investigate the effect of thermosolutal convection on the solute segregation and the nature of the flow field.

2. Modeling

We consider the vertical Bridgman growth system depicted in Fig. 1. The geometry of the computational domain is rectangular with a length/width aspect ratio equal to 10. Two isothermal zones linked by an adiabatic zone compose the temperature profile imposed on the outer wall. The cylindrical ampoule is contained in a vertical furnace and has negligible thermal mass. Solidification proceeds from the bottom of the ampoule, which is lowered vertically downward at constant velocity $V_p=10$mm/h. The melt is contained within an ampoule and bounded by a plane circular plate on top. The growth system is assumed to be steady state and perfectly axisymmetric. The ampoule is subject to heat radiation from a furnace heater and heat convection in the furnace thermal environment.

We assume that the furnace temperature varies

Table 1 Material properties of gallium-doped germanium

Property	Value
Thermal conductivity of melt(k_L)	17 W/ mK
Thermal conductivity of solid(k_S)	17 W/ mK
Heat capacity of melt(c_{pL})	0.39 kJ/kgK
Heat capacity of solid(c_{pS})	0.39 kJ/kgK
Density of melt(ρ_L)	5600 kg/m^3
Density of solid(ρ_S)	5600 kg/m^3
Melting temperature(T_m)	958 ℃
Kinematic viscosity of melt(ν)	1.3×10^{-7} m^2/s
Heat of fusion(ΔH_S)	506 kJ/kg
Thermal expansion coefficient(β_T)	0.25×10^{-3} K^{-1}
Solutal expansion coefficient(β_S)	2.15×10^{-3} wt. %$^{-1}$
Diffusivity of Ga in Ge(D)	1.3×10^{-8} m^2/s
Segregation coefficient Ga in Ge(k)	0.1

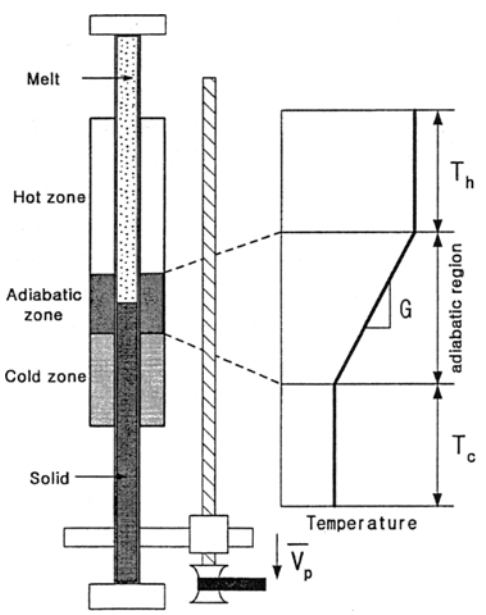

Fig. 1 Schematic of the vertical Bridgman growth system

linearly in the adiabatic zone and remains constant at the upper and lower walls. The physical properties for the melt and solid are all assumed to be constant as listed in Table 1.

The following assumptions have been employed in the development of governing equations.

1. The melt is considered to be a viscous Newtonian fluid and the flow to be incompressible and laminar.

2. Physical properties of the crystal are treated as constants except for the buoyancy term in the momentum equation, where the Boussinesq approximation is used to account for density variation with temperature and species field concentration.

3. Viscous dissipation in the energy equation is neglected.

3. Analysis

3.1 Governing equation

The governing equations of the melt and solid are obtained from the laws of conservation and are transformed in dimensionless form using the reference scaling;

$$r=\bar{r}/R,\ z=\bar{z}/R,\ u=\bar{u}/(\nu R),\ \nu=\bar{\nu}/(\nu R),$$
$$P=\bar{P}/(\rho\nu^2/R^2),\ T=(\bar{T}-T_c)/(T_h-T_c),$$
$$C=(\bar{C}-C_0)/(C_0/\kappa-C_0),\ V_p=\bar{V}_p/(\nu R)$$

In the above equations r, z, u, v, P, T, C and Vp are non-dimensional variables and R is the radius of the ampoule and C_0 is average solute concentration and Th and Tc are the temperature of the hot and cold regions of furnace. Then the governing equations in an axisymmetric domain can be expressed in conservative form as follows:

Momentum equation

$$\frac{\partial}{\partial r}\left(r\cdot u\cdot u-r\frac{\partial u}{\partial r}\right)+\frac{\partial}{\partial z}\left(r\cdot\nu\cdot u-r\frac{\partial u}{\partial z}\right)$$
$$=-r\frac{u}{r^2}-r\frac{\partial P}{\partial r} \tag{1}$$
$$\frac{\partial}{\partial r}\left(r\cdot u\cdot\nu-r\frac{\partial \nu}{\partial r}\right)+\frac{\partial}{\partial z}\left(r\cdot\nu\cdot\nu-r\frac{\partial \nu}{\partial z}\right)$$
$$=-r\frac{\partial P}{\partial z}+r\frac{Ra_T}{Pr}(T_m-T_f)+r\frac{Ra_S}{Sc}(C_m-C_0) \tag{2}$$

Energy equation

$$\frac{\partial}{\partial r}\left(r\cdot u\cdot\ T_m-r\frac{1}{Pr}\frac{\partial T_m}{\partial r}\right)+\frac{\partial}{\partial z}$$
$$\left(r\cdot\nu\cdot T_m-r\frac{1}{Pr}\frac{\partial T_m}{\partial z}\right)=0 \tag{3}$$
$$\frac{\partial}{\partial r}\left(-r\frac{a}{Pr}\frac{\partial T_S}{\partial r}\right)+\frac{\partial}{\partial z}\left(r\cdot V_P\cdot T_S-r\frac{a}{Pr}\frac{\partial T_S}{\partial z}\right)=0 \tag{4}$$

Species diffusion equation

Table 2 Definition of dimensionless variables

Dimensionless Groups	Definition	Value
Thermal Rayleigh number	$Ra_T=\frac{g\beta_T(T_h-T_c)R^3}{\nu\alpha}$	$0\text{-}1\times10^6$
Solutal Rayleigh number	$Ra_S=\frac{g\beta_S(C_0/\kappa-C_0)R^3}{\nu D}$	$0\text{-}4\times10^5$
Prandtl number	$Pr=\frac{\nu}{\alpha}$	0.01
Schmidt number	$Sc=\frac{\nu}{D}$	10

$$\frac{\partial}{\partial r}\left(r\cdot u\cdot C-r\frac{1}{Sc}\frac{\partial C}{\partial r}\right)+\frac{\partial}{\partial z}\left(r\cdot v\cdot C-r\frac{1}{Sc}\frac{\partial C}{\partial z}\right)=0 \quad (5)$$

The above equations are nonlinear in terms of the velocity, temperature and concentration fields. These fields are coupled through the convective and source terms. The four dimensionless parameters resulting from the scaling procedure are the thermal Rayleigh number, solutal Rayleigh number, Prandtl number and Schmidt number as listed in Table 2.

3.2 Boundary conditions

Along the interface, the temperature is uniform with melting temperature. Across the interface, the temperature is continuous from the assumption of thermodynamic equilibrium. The liquid concentrations at the interface are determined from the following equation. (Mcfadden and Coriell, 1987)

$$\frac{\partial C}{\partial z}=-V_pSc(1-\kappa)C,\ T=T_m \quad (6)$$

where V_p is the dimensionless translation velocity of the ampoule, κ the effective segregation coefficient and T_m is the melting temperature. Heat fluxes from the surrounding to the melt at the top, bottom and side of the cylindrical ampoule are given by,

$$-\kappa_S\frac{\partial T}{\partial z}=h_s(T-T_\infty)+\varepsilon\sigma(T^4-T_\infty^4) \quad (7)$$

where ε is the emissivity and σ is the Stefan-Boltzman constant. Symmetry conditions are enforced along the system centerline for the temperature, velocity and concentration fields.

$$u=0,\ \frac{\partial v}{\partial r}=0,\ \frac{\partial T}{\partial r}=0,\ \frac{\partial C}{\partial r}=0 \quad (8)$$

No slip conditions are imposed along the cylindrical outer melt surface, which contacts the crucible walls.

$$u=v=0 \quad (9)$$

All solid surfaces other than the solid-liquid interface are taken to be impermeable to solute.

$$\frac{\partial C}{\partial r}=0,\ \frac{\partial C}{\partial z}=0 \quad (10)$$

3.3 Numerical procedure

The governing equations with the specified boundary conditions are solved by a finite-volume method using the power law scheme and the SIMPLE algorithm in which body-fitted coordinate system has been used.

A non-uniformly spaced 31×51 and 41×61 staggered grid system are used for computation. Since there are no differences in stability and convergence of solution between two grid systems, 31×51 grid systems for melt and solid regions are employed respectively. Grids are densely deployed near the interface in order to resolve the steep gradient of solute concentration. Convergence was assumed when the residual fell below prescribed tolerance(10^{-4}). An iterative technique with the algorithm developed by Kim and Kaviany (1992) was used to determine the exact location of the interface. The balance of heat flux across the interface is the condition for determining the position of the interface. Initially the shape of interface is assumed to be flat and modified in such a way that the mass and energy conservation across the interface is exactly satisfied (Kim and Ro, 1992; Kim, 1995).

4. Results and Discussions

4.1 Interface shape

Figure 2 shows the interface shapes with varying thermal and solutal Rayleigh number.

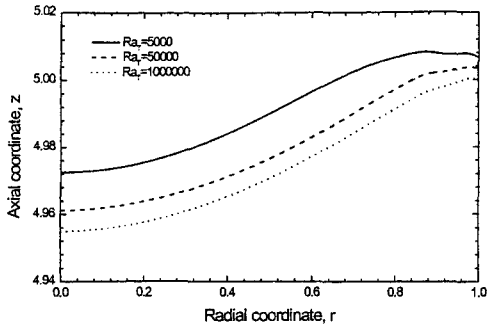

(a) Thermal convection only

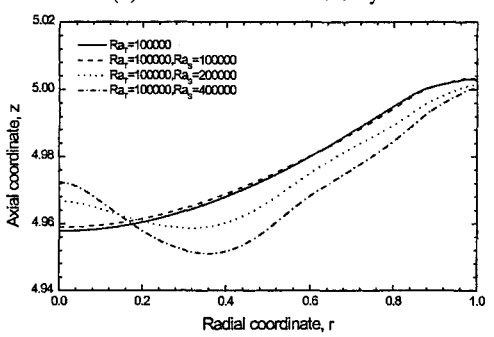

(b) Thermal and solutal convection

Fig. 2 Melt-solid interface shapes for the various thermal and solutal Rayleigh numbers

From Fig. 2(a), it is seen that the interface shape is more concave toward the crystal with the increase of thermal Rayleigh number.

For higher thermal Rayleigh numbers, the hot melt flowing down the axis of the ampoule caused the melt-solid interface to move downward. Figure 2(b) presents the comparison of the interface shapes with consideration of thermal and solutal convection. From Fig. 2(b), the interface shape for $Ra_T=1\times10^4$ and $Ra_S=1\times10^4$ is almost same as the interface calculated without solutal convection. However, the interface shapes for $Ra_S=2\times10^5$ and 4×10^5, are much different to the one in the absence of solutal convection. Thus solutal convection has a greater effect on the interface shape for higher solutal Rayleigh number.

It is striking to observe that the interface shape changes from concave to convex at the center of the ampoule with increase of the solutal Rayleigh number. This result can be explained by the secondary cell generated by solutal convection.

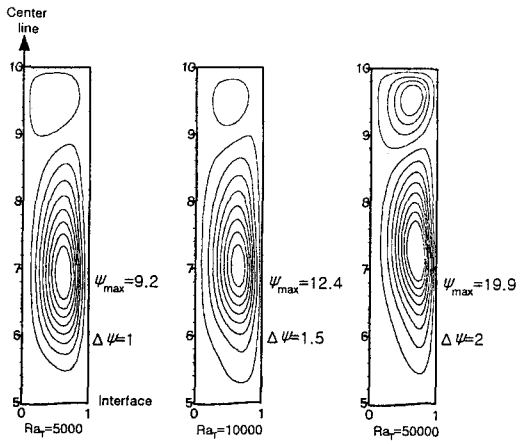

(a) Thermal convection only

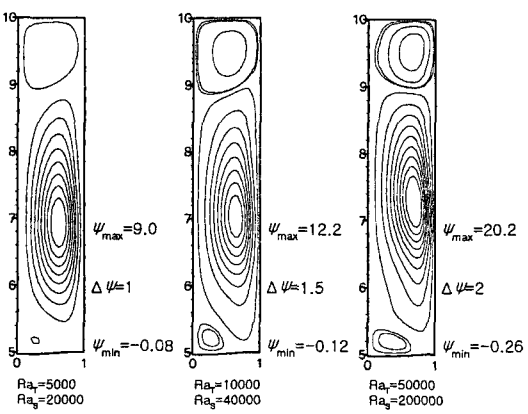

(b) Thermal and solutal convection

Fig. 3 Streamlines for various thermal and solutal Rayleigh numbers

That is, flow field has a profound effect on the interface curvature.

4.2 Flow, temperature and concentration fields

The flow fields of the melt for various thermal Rayleigh number are shown in Fig. 3(a) in which thermal convection is only considered. One flow cell is formed in liquid zone, resulting from the action of the buoyancy force induced by temperature gradients in the solution. The flow moves upward along the ampoule wall where temperature is higher and moves downward at the centerline of the ampoule where temperature is lower. As can be seen from the figure, with the increase in thermal Rayleigh number, the intensity

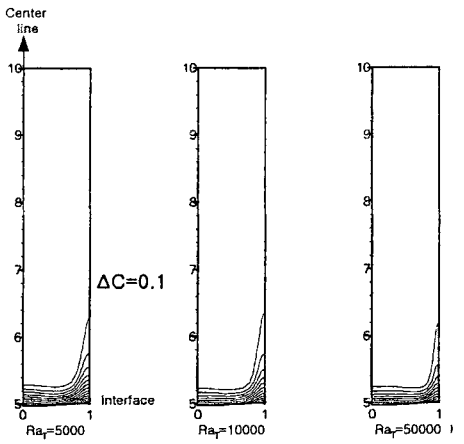

(a) Thermal convection only

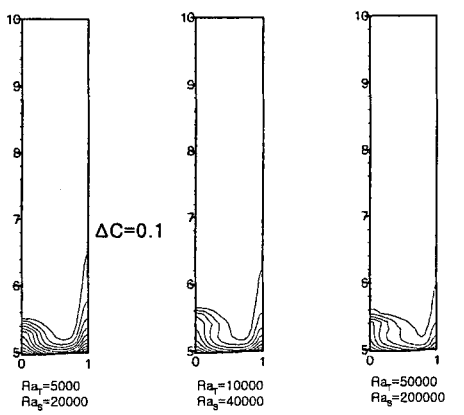

(b) Thermal and solutal convection

Fig. 4 Distribution of solute concentration for various thermal and solutal Rayleigh numbers

of convection cell becomes stronger. The center of the cell is located near the boundary of the hot and adiabatic zone (z=7) and tends to move toward the sidewall of the ampoule. Figure 3(b) shows the streamline in the melt with consideration of thermal and solutal convection. This indicates a primary convective cell rotating in a counter-clockwise manner in the melt, along with a weak secondary, clockwise convective cell driven by solute gradients adjacent to the interface. The flows in the melt are characterized by the multi-cell structure with a large vortex in the middle portion of the melt that flows downward along the centerline and a smaller vortex rotating in the opposite direction which is located near the solid-liquid interface and upper region.

Figure 4(a) shows the solute concentration distribution predicted by the calculation for various thermal Rayleigh numbers. As the crystal solidifies, solute is rejected at the interface and the level of solute near the interface increases, leading to the formation of a solute boundary layer.

The solute concentration is almost uniform in the bulk and confines concentration gradients to the interface where convection is weak. Due to the low partition coefficient (k=0.1) for gallium doped with germanium, a solute boundary layer forms in the melt adjacent to the interface. With the increase of thermal Rayleigh number, the secondary flow influences the solute distribution by convective transport and the gradient of solute concentration at the wall becomes greater. A uniform concentration cores in the interior and steep concentration gradients near the sidewall are formed as a result of convection. Since the diffusivity of germanium in gallium solution is low, the fluid flow makes important contribution to the mass transport. Figure 4(b) shows the concentration distribution in the melt when both thermal and solutal convection are considered. The solute distribution near the interface is strongly affected by the clockwise rotating secondary cell so that iso-contours of solute concentration are greatly distorted. The formation of the secondary cell causes additional, convection-based segregation to occur such that the concentration values near the center of ampoule are higher than those at the bottom. The shape of the isotherms in the melt is shown in Fig. 5.

The temperature field in the melt shows only small radial gradients and the melt isotherms are nearly flat except in the vicinity of the ampoule wall. It is observed that the thermal field in the bulk of the melt is not strongly affected by increase of the Rayleigh number. The fact that the temperature field is almost flat means that the melt is thermally stratified and indicates that heat conduction is dominant heat transfer mechanism in the melt.

The Prandtl number based on the thermal properties is 0. 01, which represents the sensitivity of temperature distribution. The isotherm flatness is important since it gives rise to uniform solute

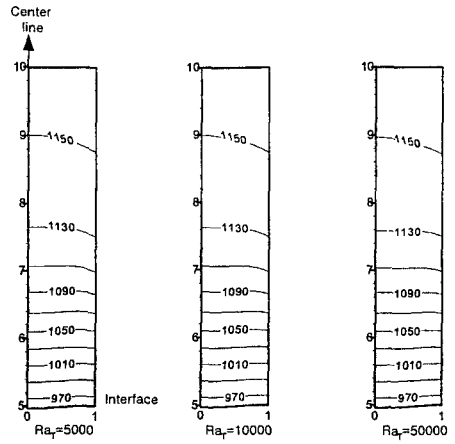

(a) Thermal convection only

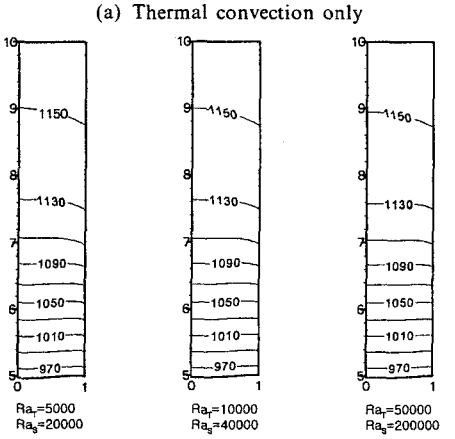

(b) Thermal and solutal convection

Fig. 5 Temperature distribution in the melt for various thermal and solutal Rayleigh numbers

distribution along the interface, which is desirable for crystal growth.

4.3 Radial concentration along the interface

From Fig. 6(a) it is observed that the distribution of solute along the interface greatly depends on the thermal Rayleigh number. In other words, melt flow near the interface changes the characteristics of the radial distribution of concentration. As the thermal Rayleigh number increases, the location of maximum concentration is moved from the sidewall to the center of the ampoule. This is due to the existence of secondary cell caused by thermal convection at the high Rayleigh number. Figure 6(b) shows the radial distribution of solute concentration along the

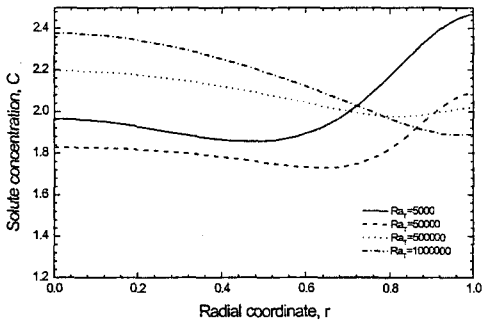

(a) Thermal convection only

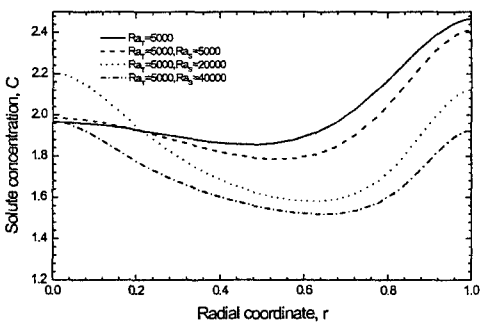

(b) Thermal and solutal convection

Fig. 6 Solute concentration along the interface for various thermal and solutal Rayleigh numbers

melt-solid interface in the presence of thermal and solutal concentration. Radial segregation is observed due to the transport of solute under the action of thermosolutal convection.

Although the values of the flow velocity due to solutal convection are small, the influence on the solute distribution is significant. The solute distribution for low solutal Rayleigh number is more uniform than that for high solutal Rayleigh number. Nonuniformity results from the existence of two counter-rotating cells near the interface.

5. Conclusions

Numerical simulations of the vertical Bridgman crystal growth at various thermal and solutal Rayleigh number have been performed to analyze the influences of the thermosolutal convection on the heat and mass transfer as well as interface shapes during growth of gallium dope with germanium. Generally speaking, thermosolutal convection has a little influence on the interface

shape for low solutal Rayleigh number. However, significant deviation of interface shape can be found at the high thermal and solutal Rayleigh number. Also the fluid flow and solute concentration field depends on the thermal and solutal Rayleigh number, but the temperature field does not change significantly with respect to the thermal and solutal Rayleigh number.

Secondary flow near the interface plays an important role in concentration distribution in the melt. The results from these simulations show that the influence of thermosolutal convection on solute profiles along the interface during the process is significant.

References

Carlson, F. M., Fripp, A. L. and Crouch, R. K., 1984, "Thermal Convection during Bridgman Crystal Growth," *J. Crystal Growth*, Vol. 68, pp. 747~751.

Chang, C. and Brown, R. A., 1983, "Radial Segregation Induced by Natural Convection and Melt/Solid Interface Shape in Vertical Bridgman Growth," *J. Crystal Growth*, Vol. 63, pp. 343~364.

Dutta, P. S., Bhat, H. L. and Kumar, V., 1995, "Numerical Analysis of Melt-Solid Interface Shapes and Growth Rates of Gallium Antimonide in a Single-Zone Vertical Bridgman Furnace," *J. Crystal Growth*, Vol. 154, pp. 213~222.

Kim, C. J. and Kaviany, M., 1992, "A Fully Implicit Method for Diffusion-Controlled Solidification of Binary Alloys," *Int. J. Heat Mass Transfer*, Vol. 35, No. 5, pp. 1143~1154.

Kim, M. G., 1995, "Effects of Rotation on the Czochralski Silicon Single Crystal Growth," *Transactions of the Korean Society of Mechanical Engineers*, Vol. 19, No. 5, pp. 1308~1318.

Kim, M. G. and Ro, S. T., 1992, "Analysis of Solidification Process around a Vertical Tube Considering Density Change and Natural Convection," *Transactions of the Korean Society of Mechanical Engineers*, Vol. 16, No. 1, pp. 142~155.

Kuppurao, S. and Derby, J. J., 1997, "Designing Thermal Environments to Promote Convex Interface Shapes during the Vertical Bridgman Growth of Cadimuim Zinc Telluride," *J. Crystal Growth*, Vol. 172, pp. 350~360.

McFadden, G. B. and Coriell, S. R., 1987, "Thermosolutal Convection during Directional Solidification. II. Flow transitions," *Phys. Fluids Vol.* 30, No. 3, pp. 659~671.

Ouying, H. and Shyy, W., 1997, "Numerical Simulation of CdTe Vertical Bridgman Growth," *J. Crystal Growth*, Vol. 173, pp. 352~366.

Xiao, Q., Kuppurao, S., Yeckel, A. and Derby, J. J., 1996, "On the Effects of Ampoule Tilting during Vertical Bridgman Growth: Three-Dimensional Computations via a Massively Parallel, Finite Element Method," *J. Crystal Growth*, Vol. 167, pp. 292~304.

Xing, Y., Tabarrok, B. and Walsh, D., 1996, "The Influence of Thermal Convection on CdTe Growth by the Traveling Heater Method," *J. Crystal Growth*, Vol. 169, pp. 704~714.